Effect of Electrochemical Potential and Solution Concentration on the SCC Behaviour of X-70 Pipeline Steel in NaHCO₃

A. Torres-Islas[1,], J. G. González-Rodríguez[1]*

[1] UAEM, Centro de Investigacion en Ingeniería y Ciencias Aplicadas Av. Universidad 1001, Col. Chamilpa, 62210 Cuernavaca, Mor., México
[*]E-mail: atimarquis93@yahoo.com.mx

The stress corrosion cracking (SCC) behaviour of a X70 microalloyed pipeline steel, with different heat treatments under both anodic and cathodic overpotrentials has been evaluated by using of the slow strain rate testing (SSRT) technique at 50ºC. Heat treatments included the as-received (annealed) condition and water quenched. Tests solutions consisted of 0.1, 0.05, 0.01 and 0.005 M sodium bicarbonate (NaHCO₃). Hydrogen permeation measurements were also carried out. Additionally, experiments using the SSRT technique with pre-charged hydrogen samples and potentiodynamic curves at different sweep rates were also done to elucidate hydrogen effects in this type of steel. Results showed that the steel under both heat treatments was highly susceptible to SCC only in 0.005 M NaHCO₃ and with the application of anodic or very high cathodic overpotentials. The quenched steel, with a martensitic microstructure, was always more susceptible to SCC than the steel in the as received condition with a ferritic-pearlitic microstructure. Hydrogen permeation tests showed a much higher hydrogen uptake by the quenched than the as-received steel. Pre-charging tests showed that only the quenched specimen was susceptible to fail by a hydrogen-based mechanism, whereas low and fast sweep polarization curves showed that the steel in the as-received condition was more susceptible to fail by an anodic dissolution-based SCC mechanism. Thus, the SCC mechanism for the as-received steel was dominated by anodic dissolution at the free corrosion potential, E_{corr}, or with the application of anodic overpotentials, whereas for the steel in the quenched condition was dominated by a hydrogen-based mechanism. Both steels were dominated by a hydrogen-based mechanism with the application of high cathodic overpotentials.

1. INTRODUCTION

There has been a lot of controversy about the transgranular stress corrosion cracking (TGSCC) that pipelines can develop under normal operating conditions when a coating breaks down and ground

water comes into contact with the outside surface. Recently, Parkins[1], studying the stress corrosion cracking (SCC) behavior of X-52, 60 and 65 steels in diluted near-neutral solutions, has suggested that, even when there is evidence of the ingress of hydrogen to steels at potentials around the free corrosion potential (E_{corr}) values, there was also evidence of dissolution occurring simultaneously. He observed that, even for solutions involving TGSCC of pipeline steels, hydrogen entry can occur and is involved in the crack growth process, however, hydrogen-induced cracking is not exclusively involved since there is ample evidence of dissolution being associated with cracking.

Since the first TGSCC observed in the Trans Canada Pipe Lines Ltd. in 1985, many other countries such as Italy, Mexico and the former Soviet Union have experienced such a failures. Intergranular stress corrosion cracking (IGSCC) of pipelines can also occur in highly concentrated bicarbonate-carbonate (HCO_3/CO_3^{2-}) solution with high pH (~9-11). This type of SCC occurs in a very restricted range of electrochemical potentials (-550 mV vs a saturated calomel electrode [SCE] to ~-650 mV_{SCE}. Dominated by film rupture and dissolution, this is so-called classical SCC [2-4]. Several instances of TGSCC were detected recently at coating disbonding areas of Canadian pipelines [5,6]. Many researchers are focusing more attention on this new SCC phenomenon because it is associated with much lower HCO_3/CO_3^{2-} concentrations with small quantities of KCl, $CaCl_2$ and $MgSO_4 \cdot 7H_2O$ and pH values, from 5.5 to 7.5,lower than those at which classic SCC occurs. Many efforts have been made to understand the mechanism of this SCC in this non-classic environment [7-18]. For instance, Fang et al. [8] used the slow strain rate testing (SSRT) technique to study the mechanical and environmental effects on SCC of an X-70 pipeline steel in diluted near neutral pH applying different electrochemical potentials. They found that cracking occurred at high cathodic potentials and low strain rates. Lu [14] studied the relationship between yield strength and near-neutral pH SCC resistance of pipeline steels (X-52, X-70, X-80 and X-100). He found that the SCC resistance decreased with strength level but it was greatly affected by microstructure. Chu [17] studied the microstructure dependence of SCC initiation in X-65 pipeline steel exposed to a near-neutral soil environment. He found that micro cracks initiated mostly from pits at metallurgical discontinuities such as grain boundaries, pearlitic colonies, and banded phases in the steel. Finally, He [18], using hydrogen permeation tests, studied the effect of cathodic potential on hydrogen uptake by X-65 pipeline steel exposed to a near-neutral pH soil solution, finding that the hydrogen content increased with a decrease in the cachodic potential but it decreased when a calcium carbonate film was formed. The objective of this work was to study the effect of different heat treatments and, thus, microstructure, in conjunction with the effect of electrochemical potential and solution concentration on the SCC resistance of a pipeline steel in $NaHCO_3$ solutions using the slow strain rate testing (SSRT) technique.

2. EXPERIMENTAL PART

The material used was an X-70 pipeline steel, with composition as specified in Table 1. To quench the steel, specimen was heated at 850°C during 40 minutes and then water quenched in static water. Cylindrical tensile specimens with a 25.00 mm gauge length and 2.50 mm gauge diameter were

machined from an unused pipeline perpendicular to the rolling direction. Before testing, the specimens were abraded longitudinally with 600-grade emery paper, degreased, and masked, with the exception of the gauge length.

Table 1. Chemical composition of X-70 pipeline steel (wt.%)

C	Mn	Si	P	S	Al	Nb	Cu	Cr	Ni	Mo	Ti	Fe
0.027	1.51	0.1	0.014	0.002	0.035	0.093	0.28	0.27	0.16	0.004	0.011	Bal.

Specimens were subjected to conventional, monotonic SSRT testing in air as an inert environment, and in 0.1, 0.05, 0.01 and 0.005M NaHCO$_3$ solution at 50 ºC at a strain rate of 1.36 x10^{-6}s^{-1}. Tests were done at the open circuit potential, E$_{corr}$, and also applying potentials 100, 200, and 300 mV more anodic and 100, 200, 600, and 1600 mV more cathodic that E$_{corr}$. The loss in ductility was assessed in terms of the percentage reduction in area (%R.A) by using:

$$\%R.A. = \frac{A_i - A_f}{A_i} \times 100 \qquad (1)$$

where A$_i$ and A$_f$ are the initial and final area respectively. A susceptibility index to SCC (I$_{SCC}$) was calculated as follows:

$$I_{SCC} = \frac{RA_{AIR} - RA_{SOL}}{RA_{AIR}} \qquad (2)$$

where RA$_{AIR}$ and RA$_{SOL}$ are the percentage reduction in area values in air and in the NaCO$_3$ solution respectively. Thus, the closer the I$_{SCC}$ value to the unit, the more susceptible the specimen was towards SCC. The fracture surfaces were then examined using scanning electron microscopy (SEM). Some specimens were pre-charged with hydrogen and strained to rupture in air. The pre-charging with hydrogen was done in 0.5M Sulfuric acid (H$_2$SO$_4$) with a cathodic current density of 0.1 mA/cm^2 during 60 minutes. Potentiodynamic polarization curves were performed at a sweep rate of 1 mV/s using a fully automated potentiostat controlled with a desk top computer. Additionally, to evaluate the SCC susceptibility of the steel by film rupture some tests were performed at 10 mV/s (fast scan). All potentials are referred to the saturated calomel electrode (SCE). A graphite rod was used as auxiliary electrode. The test solutions were prepared from analytical grade chemicals.

Hydrogen permeation tests were carried out by using the two-component Devanathan-Stachurski[19] cell. The specimen, 0.5 mm thick, was mounted between the two compartments, giving an effective area of 3.14 cm^2 exposed to the NaCO$_3$ solution, under open circuit conditions to generate hydrogen. The hydrogen collection compartment contained an electrolyte of 0.5 M Sodium Hydroxide (NaOH) solution purged with nitrogen (N$_2$) gas. The palladium (Pd)-plated specimen surface exposed

to this solution was potentiostatically passivated at a constant potential of +300 mV. The test solutions were prepared from analytical grade chemicals. All tests were performed at 50°C.

3. RESULTS

3.1. Microstructures

The microstructures produced by the different heat treatments are shown in Fig. 1. The microstructure of the as received sample show bands of ferrite alternated with bands of cementite as can be observed on Fig. 1 a, it was also found a fine dispersion of precipitates. The samples quenched in water (Fig. 1b), presents a typical structure of martensite with massive segregation at the martensitic lath boundaries and colonies of pearlite; fine dispersion of precipitates is observed.
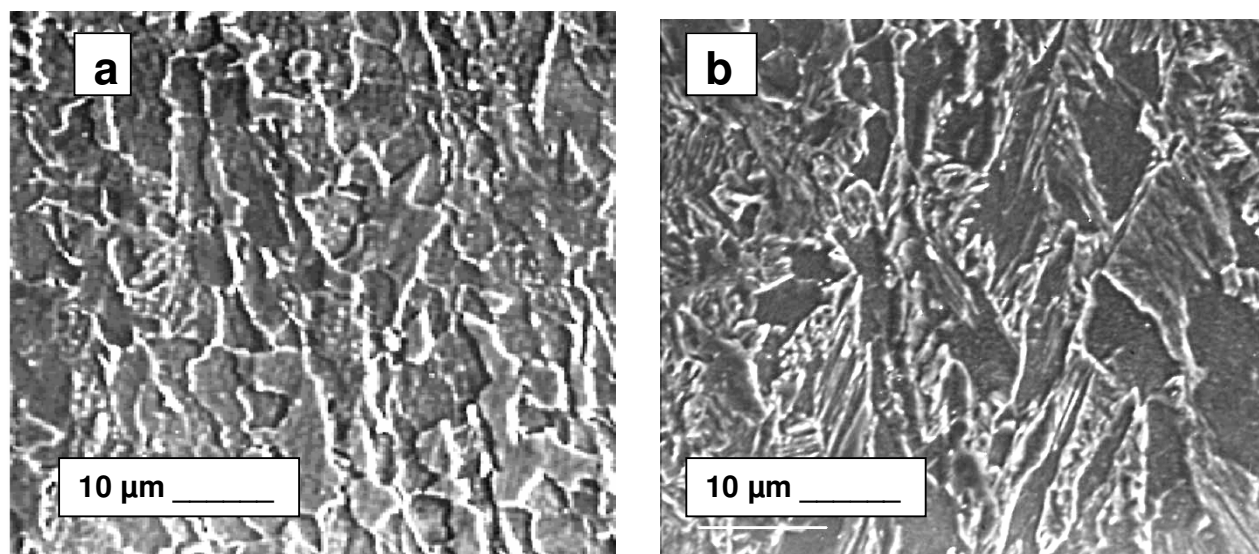
Figure 1. Microestructures of the X-70 steel showing the a) as-received, b) quenched condition

3.2. Effect of NaHCO₃ Concentration on the Polarization curves

Fig. 2 shows polarization curves of the steel in the as-received condition in NaHCO₃ at different concentrations. The shape of the polarization curves changed with HCO_3^- concentration in terms of the presence of a passive region. Even in the most diluted solution, there was evidence of a passive region. The E_{corr} value was between around –400 mV regardless the solution concentration. There was no a clear effect on the potential at which the passive region started (E_{pass}), however, the pitting potential, E_{pit}, increased as the solution concentration decreased. Similarly, the passive current density (i_{pass}) increased as the solution concentration was increased. For the most diluted solution,

some instabilities were observed in the passive zone, instabilities which were more pronounced as the potential approached the E_{pit} value. These instabilities may be attributed to the breakdown of the passive film and a rebuilding of the same. It was not very clear which of the two most concentrated solutions produced the highest corrosion current density value, i_{corr}, however, it was very clear that the lowest i_{corr} value was observed in the most diluted solution. The difference between the lowest and the highest i_{corr} value was less than five times.
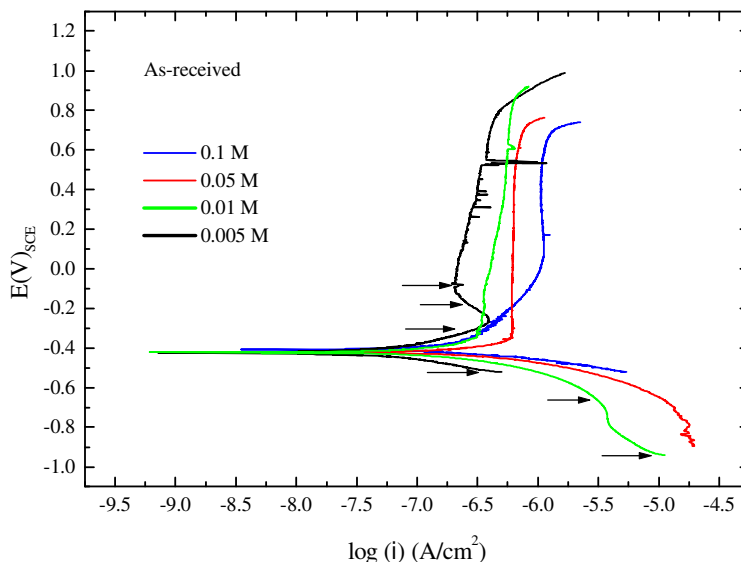

Figure 2. Effect of the $NaHCO_3$ concentration on the polarization curves for the as-received X-70 steel. Arrows indicate the potentials, close to E_{corr}, at which SSRT tests were performed.

On the other hand, for the quenched specimen, Fig. 3, the situation was quite different, since in the most diluted solution, the specimen did not show a passive region, whereas in the other solutions, the specimen did show a passive region. The lowest E_{corr} and i_{corr} values were observed in the most diluted solution (0.005M) whereas the highest E_{corr} and i_{corr} values were obtained in the 0.1M solution. This time, no instabilities were observed in the passive zone in none of the solutions. The highest E_{pit} value was observed in the 0.05M solution concentration, whereas the lowest value was for the 0.01M solution. Finally, the highest anodic current density was observed for the most diluted solution, whereas the highest passive current density, i_{pass}, was obtained in the 0,1M solution concentration. Is worthy to note that, in the most diluted solution, i.e. 0.005M, the i_{corr} value for the quenched specimen, around 10^{-6} A/cm^2, was ten times higher than that for the as-received sample, which had a value close to 10^{-7}A/cm^2.
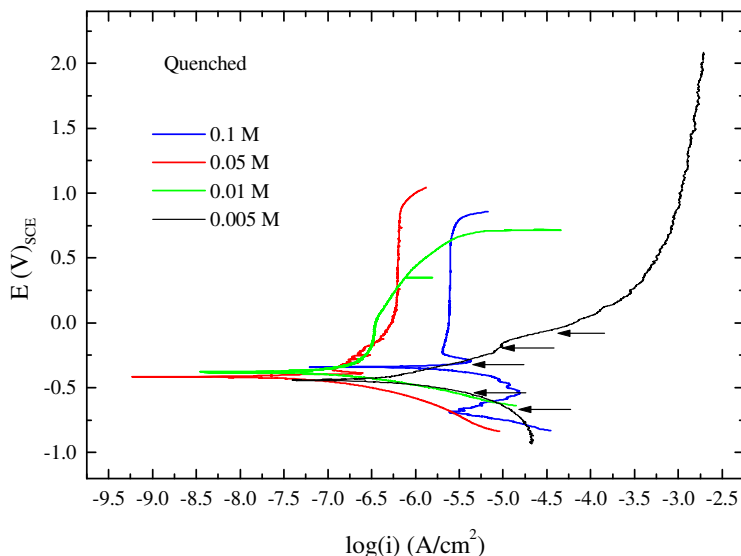
Figure 3. Effect of the NaHCO$_3$ concentration on the polarization curves for the quenched X-70 steel. Arrows indicate the potentials, closest to E$_{corr}$ at which SSRT tests were performed.

3.3. Slow Strain Rate Tests

The effect of the solution concentration on the susceptibility towards SCC, I$_{SCC}$ is shown in Fig. 4. This figure shows that the susceptibility to fail by SCC, in both heat treatments, increases as the solution concentration decreases, especially for the quenched specimen, which had the highest I$_{SCC}$ value in the most diluted solution. The tendency of the steel to fail by SCC by film rupture was evaluated on the basis that at least 1 order of magnitude difference in current density between the slow and the fast sweeps [20,21], at 1 mV/s and 10 mV/s respectively.
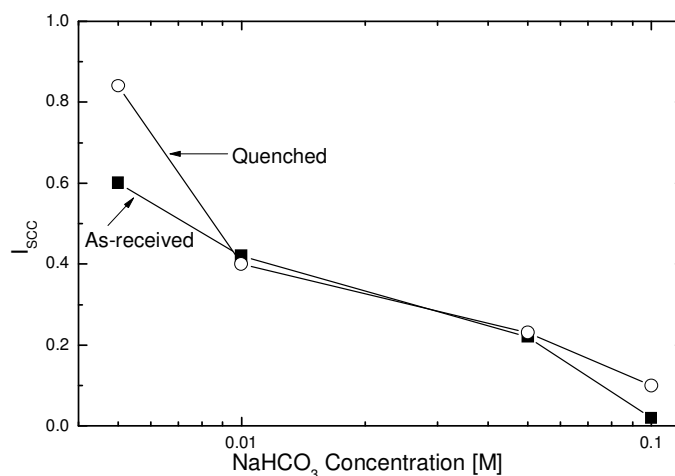

Figure 4. Effect of the NaHCO$_3$ concentration on the I$_{SCC}$ index value for the X-70 steel in the as-received and the quenched condition.

The results of the i_{pass} values in the active-passive region for the different heat treatments using slow and fast seeps are given in Table 2. Table 2 shows that, the steel in the as-received condition shows 1 order of magnitude difference in current density between the slow and the fast sweeps, whereas the quenched specimen did not show a passive behavior in this solution neither in the fast nor in the slow sweep rate. Therefore, the steel in the as-received condition was much closer to meet the requirements required to fail by SCC by the film rupture mechanism.

Table 2. Effect of Heat Treatment on the i_{pass} values obtained using fast and slow sweeps in 0.005 M $NaHCO_3$

Heat treatment	$i_{pass}(A/cm^2)$ at Slow Scan	$i_{pass}(A/cm^2)$ at Fast Scan	Ratio
As-received	$10^{-7.75}$	$10^{-6.5}$	18
Water-quenched	No passive region	---	

To give a better insight on this, some specimens were pre-charged with hydrogen and then ruptured in air. The I_{SCC} values are given on table 3, which shows that the steel in the as-received condition did not show a tendency to fail by SCC under these conditions, whereas the quenched specimen had a very high tendency to fail by SCC once both specimens have been pre-charged with hydrogen.

Table 3. I_{SCC} values for specimens pre-charged with hydrogen and fractured in air.

Heat Treatment	I_{SCC}
As-received	0.14
Water quenched	0.92

The effect of the applied potential upon the I_{SCC} value is given on Fig. 5. It can be seen that regardless the heat treatment, the highest susceptibility to fail by SCC is obtained applying very high cathodic overpotentials. Intermediate I_{SCC} values were obtained either at the free corrosion potential, E_{corr}, or by applying anodic potentials. Finally, the lowest susceptibility towards failure by SCC was obtained by applying mild cathodic over potentials, either 100 or 200 mV more negative than E_{corr}. It should be noted that, in all cases, the tendency to fail by SCC was higher for the quenched than for the as-received steel.
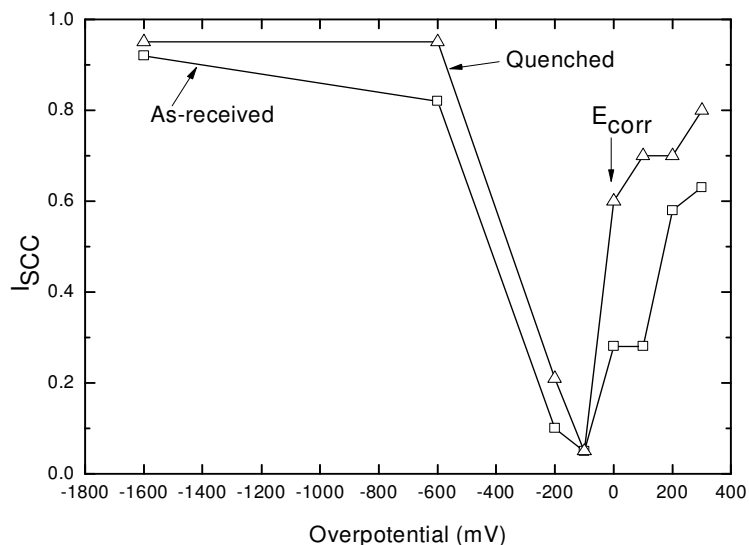
Figure 5. Effect of electrochemical overpotential on the I_{SCC}, for X-70 pipeline steel in 0.005 M $NaHCO_3$ at 50 ºC.

A cross section of the as-received and quenched specimen steel fractured in 0.005M $NaHCO_3$ at E_{corr} is shown in Fig. 6 , where the evidence of corrosion products inside the cracks is evident in both cases. It should be noted that, in both cases, the crack tip is not covered by the corrosion products but only the crack walls.
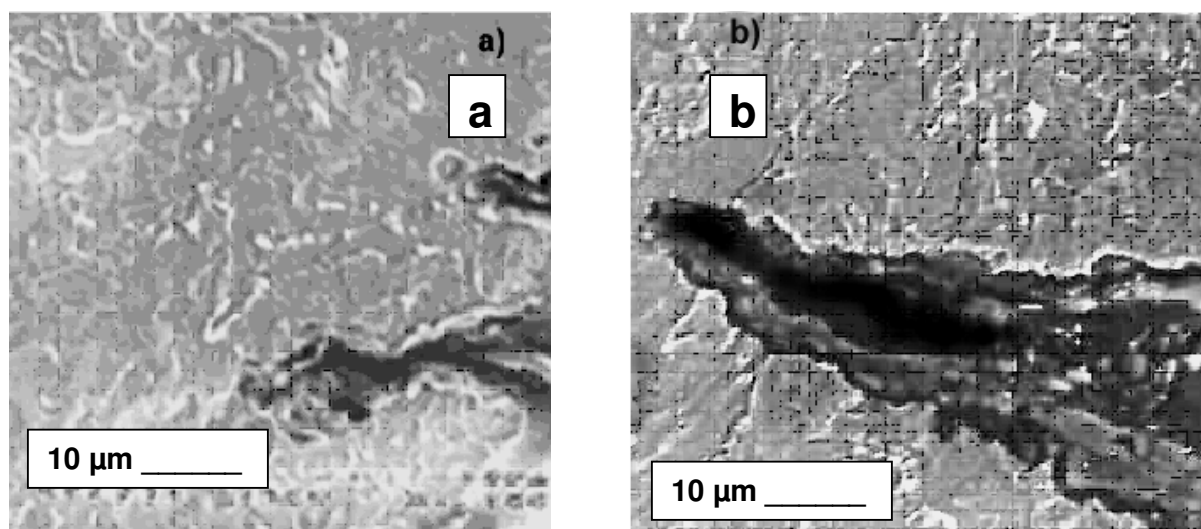

Figure 6. Cross section micrograph of the a) as-received and b) quenched steel fractured in 0.005M $NaHCO_3$ solution at E_{corr}

A micrograph of the as-received steel which failed by applying 100 mV more anodic and 1600 more cathodic than E_{corr} is shown on Fig. 7 a and b respectively. In both cases it can be seen that the cracks are transgranular, but whereas the crack found in the specimen which failed by applying an anodic overpotential was full of corrosion products, these were absent inside the crack found in the specimen under a cathodic overpotential.
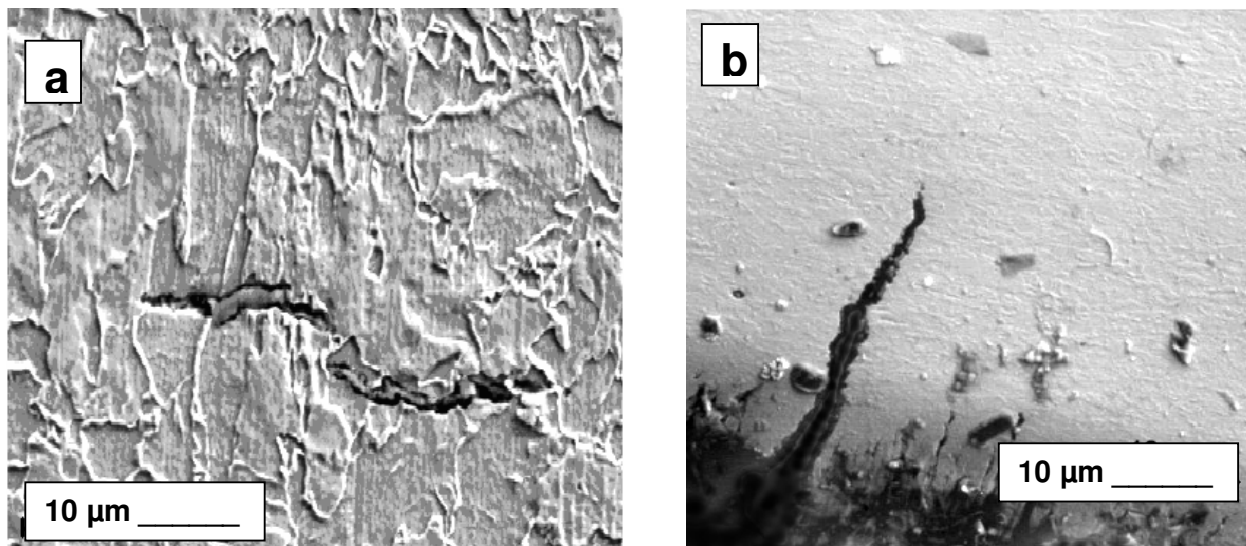

Figure 7. Secondary crack in the as-received steel applying a) +100 and b) -1600 mV in 0.005M NaHCO$_3$ solution at 50 ºC
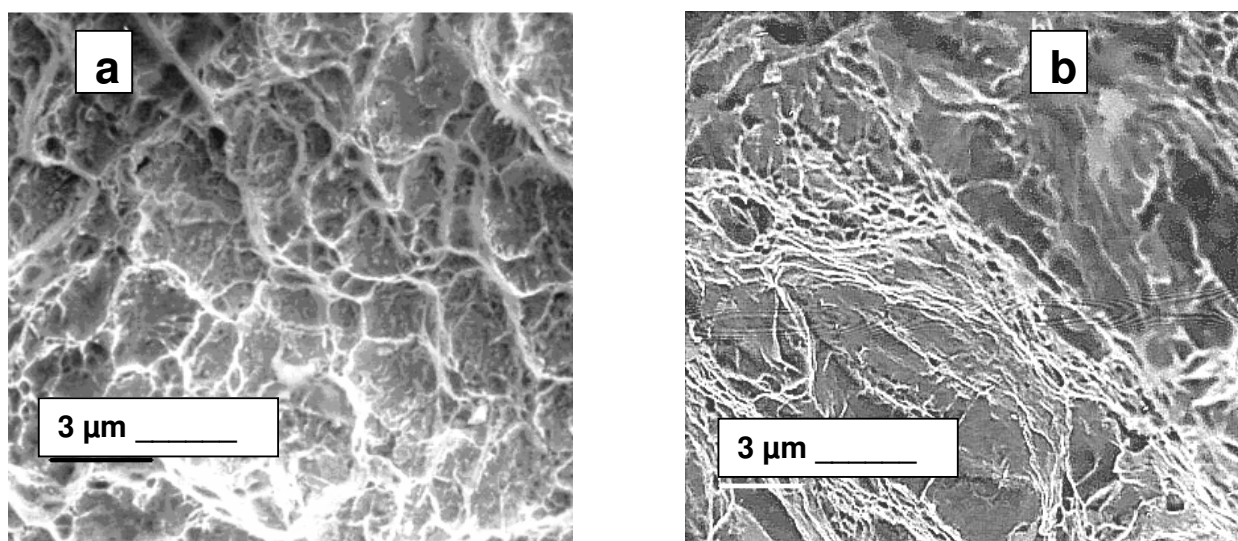

Figure 8. Fracture surface of (a) as-received and (b) pipeline quenched X-70 steel fractured applying -1600 mV

Finally, Fig. 8 shows a micrograph of the as-received and quenched specimens, which failed with the application of 1600 mV more cathodic than E_{corr}. Even when the as-received steel shows transgranular cracks, there is evidence of plastic deformation, whereas the quenched steel showed brittle type of fracture, with the river-bed shaped crack orientation.

The effect of solution concentration on the hydrogen permeation current density, J, for the as-received steel is shown on Fig. 9. It can be seen that the steady state hydrogen permeation current density value increases as the solution concentration decreases, obtaining the lowest value in the most diluted solution and the highest value, more than two orders of magnitude, in the most concentrated solution, i.e 0.005 M NaHCO$_3$.
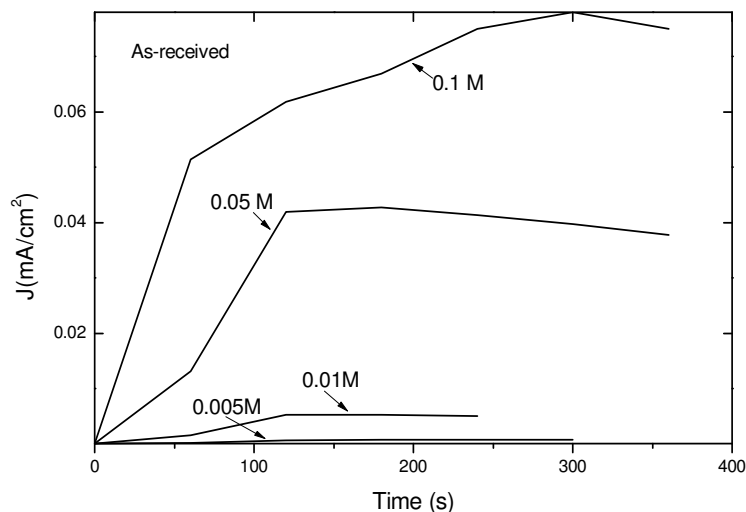

Figure 9. Effect of the NaHCO$_3$ solution concentration on the hydrogen permeation current density for X-70 pipeline steel in the as-received condition.
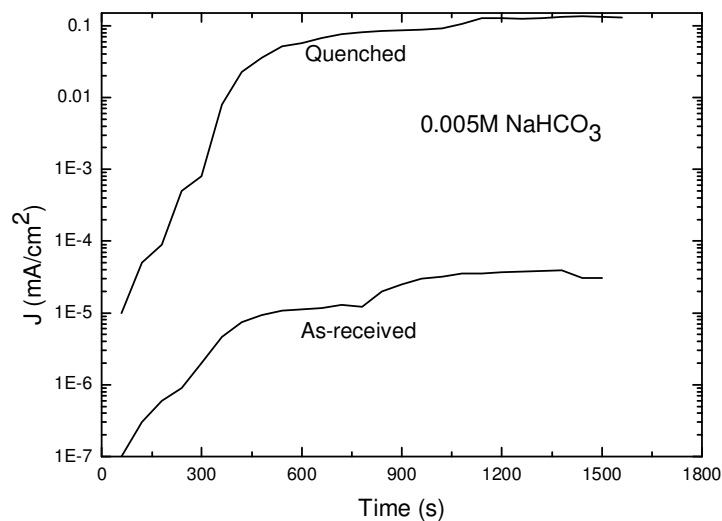

Figure 10. Effect of heat treatment on hydrogen permeation current density for X-70 pipeline steel in 0.005 M NaHCO$_3$ solution.

On the other hand, the steady state hydrogen permeation current density value was much higher, four orders of magnitude, for the quenched condition than that for the as-received specimen, Fig. 10.

4. DISCUSSION

The cathodic and anodic reactions of X-70 steel in $NaHCO_3$ solutions are reduction of hydrogen ions and oxidation of iron:

$$H^+ + e^- \rightarrow H \qquad (3)$$

$$Fe \rightarrow Fe^{2+} + 2e^- \qquad (4)$$

with an increase in the Fe^{2+} ions concentration. Hydrolysis of water by

$$Fe^{2+} + H_2O \rightarrow Fe(OH)^- + H^+ \qquad (5)$$
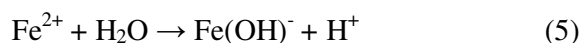
will cause an increase in the H^+ ions concentration with a further decrease in the pH inside the crack. Due to the presence of bicarbonate ions in solution, a layer of corrosion products of $FeCO_3$ will form and deposit on the steel surface according to

$$Fe^{2+} + HCO_3^- \rightarrow FeCO_3 + H^+ \qquad (6)$$
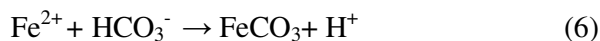
which can passivate the steel. During fast sweeping, there is not enough time for film to form on the electrode surface, generating a potential range where the steel is in an active dissolution state. On the other hand, during slow sweeping, there is sufficient time for film formation and passivate the steel, at least in the as-received condition.

In highly concentrated bicarbonate-carbonate solutions, with high pH (~9 to11) the SCC of pipelines is intergranular and is dominated by film rupture and anodic dissolution (AD). Our results, shown in Figs. 4 and 5, have shown that, regardless of the heat treatment, and, thus, the microstructure, X-70 pipeline steel is highly susceptible to SCC in diluted, 0.005M $NaHCO_3$ solutions. When these specimens were fractured in air, but pre-charged with hydrogen, the as-received specimens recovered its ductility, having low I_{SCC} value indicating that, at the open circuit potentials, this steel is not susceptible to hydrogen-enhanced SCC. Alternatively, Fig. 9 shows that, the solution concentration where the steel in the as-received condition showed the highest susceptibility to fail by SCC, 0.005M $NaHCO_3$, is precisely the solution which produces the lowest hydrogen uptake. This means that the SCC mechanism that could be occurring in the as-received specimen is anodic dissolution, since charging with hydrogen induced a recovery in their ductility. This was also evidenced when the tendency to SCC to occur by film rupture was evaluated at slow and fast sweeps [20,21]. The difference of one order of magnitude in the obtained passive current density between the slow and fast sweeps (Table 2) means that only in the as-received condition the steel will fail by SCC by anodic

dissolution. According to Parkins [21], during fast sweeping, there is not enough time for film to form on the electrode surface, generating a potential range where the steel is in an active dissolution stae. On the other hand, during slow sweeping, there is sufficient time for film formation and passivate the steel. This work shows that the steel in the as-received condition experience active dissolution and passivation but not in the quenched condition. Thus, anodic dissolution reaction plays a significant role in the SCC of X-70 steel in the as-received condition in diluted NaHCO$_3$ solutions. The presence of corrosion products at the crack walls but not at the crack tip, Fig. 6 a, supports this. Thus, at the free corrosion potential, SCC of X-70 steel in the as-received condition is controlled by anodic dissolution but not by hydrogen involvement. Polarization curves shown on Fig. 2 shows that, at 100 mV more anodic than E$_{corr}$, the steel is in the active state, and therefore dissolution of the metal is occurring. At 200 and 300 mV more anodic then E$_{corr}$ the steel is at the onset of passive state, therefore the passive film is too weak and easily to be disrupted by straining, allowing the crack tip to corrode. Hydrogen permeation measurements did show evidence of too much hydrogen on these conditions. As the applied electrochemical potential is made more cathodic, more hydrogen atoms are formed, and thus, the probability to penetrate into the steel to induce brittle type of failure is higher.

On the other hand, pre-charging with hydrogen and straining the specimens in air only induced brittle type of fractured in the quenched condition. Polarization curves for this specimen did not show the presence of a passive film in the solution which induced SCC, i.e. 0.005M NaHCO$_3$. The slow and fast sweep test shows that the steel in the as-received condition experience active dissolution and passivation but not in the quenched condition. Hydrogen permeation showed that the hydrogen uptake by X-70 in the quenched condition showed was much higher, four orders of magnitude, than that for the as-received condition. However, there was evidence of corrosion taking place when these specimens failed by SCC, see Fig. 6 b, it means that, perhaps, even when is evident that is hydrogen which is inducing the cracking on this steel, dissolution of the steel is necessary to corrode the metal and produce hydrogen. It is expected, then, that hydrogen atoms will penetrate the steel, in the quenched condition, and get involved in the cracking mechanism. To further confirm this, locking at the polarization curves shown on Fig. 3, the steel does not show a passive behavior, and at the anodic applied potentials (100, 200 and 300 mV more anodic than E$_{corr}$) shown with arrows, the steel is in the anodic dissolution state. It has been shown that, even under conditions that favors anodic dissolution, the electrochemical conditions inside the pits are such that hydrogen discharge is possible. Hydrogen permeation measurements shown on Fig.10 have shown this suggesting dissolution and hydrogen ingress into the steel. The dissolution rates at the cracks tips are high enough to cause the crack walls to passivate, providing a large cathode inside the crack, coupled to a small anode at the crack tip where film rupture took place.

The fact that the quenched steel was most susceptible to SCC is due to that coarsening microstructural phases such as martensite or bainite are highly stressed microstructure because of the excess carbon trapped interstitially[18] while fine ferrite and cementite are less susceptible to SCC. The different heat treatments given to the steel cause alteration in its microstructures, resulting in different SCC susceptibilities. This work has shown that martensite was more susceptible to SCC than ferrite. Hence, it is assumed that grain boundaries carbon segregation coupled with severe internal stresses will render grain boundaries susceptible to stress corrosion crack propagation. So, it is

expected that, under these conditions, the cracking propagation would be mainly intergranular. In this work, we were not able to detect intergranular craking as evidenced by Figs. 6-8. However, as we pointed it out in our introduction, in the non classical SCC found in lower carbonate/bicarbonate solutions, the SCC propagation was transgranular, as opposed to the intergranular SCC found in highly concentrated carbonate/bicarbonate solutions. In the as-quenched condition, it is expected that carbon segregation at grain and interlath boundaries combined with an internally stressed martensite will give rise to an increasingly susceptible steel condition. When crack growth is mainly by hydrogen embrittlement (HE), it is apparent that the distribution and type of hydrogen traps in the form of inclusions and second phases play a key role on the overall steel susceptibility. Among the microstructural features that can act as noxious traps of hydrogen are inclusions and segregation bands containing lower-temperature products (bainite and martensite).

5. CONCLUSIONS

1.- SSRT results showed that X-70 steel is immune towards SCC in concentrated $NaHCO_3$ solutions, but it was highly susceptible to SCC in the most diluted concentration, 0.005M $NaHCO_3$ solution, at 50 ºC , regardless the heat treatment.

2.-The quenched steel was the more susceptible to SCC in 0.005M $NaHCO_3$ than the steel in the as-received condition.

3.-The mechanism of SCC in X-70 pipeline steel in 0.005M $NaHCO_3$ solutions was dominated by film rupture and anodic dissolution in the as-received at the free corrosion potentials and with the application of anodic overpotentials.

4.-For the quenched, it seems that the SCC mechanism is dominated by hydrogen embrittlement assisted by anodic dissolution at E_{corr} or with the application of anodic potentials.

5.-For both heat treatments, the SCC mechanism under the application of cathodic overpotentials was dominated by a hydrogen-based mechanism

References

1. R.N. Parkins, J.A. Beavers, *Corrosion,* 59 (2003) 258
2. J.M. Sutcliffe, R.R.Fessler, W.K. Boyd, R.N. Parkins, *Corrosion* 28 (1972) 313
3. A.K. Pilkey, S.B. Lambert, A. Plumtree, *Corrosion*, 51(1995)139
4. J.Might, D.J.Duquete, *Corrosion*, 52 (1996) 428
5. B.Delanty, J. O´Beirne, *Oil Gas J*, 20 (1985) 139

6. R.H. Justice, J.D. Mackenzie, "Progress in the Control of Stress Corrosion Cracking in a 914-mm OD Gas Transmission Pipeline", Proc. NG-19/EPRG 7th Biennial Joint Mtg on Line Pipe Research, Pipeline Research Commitee of the American Gas Association, paper No.28 (Arlington, VA:AGA, 1988).
7. B.Y. Fang, E.H. Han, J.Q. Wang, W.Ke *Corroson Eng. Sci. and Technology* , 42 (2007) 123
8. B. Fang, E.H. Han, J. Wang, W. Ke *Corrosion*, 63 (2007) 419
9. B.W. Pan, X. Peng, W.Y. Chu, Y.J. Su, L.J. Qiao, *Mat. Sci. Eng*. 76 (2006) 434
10. J.T. Bulger, B.T. Lu, J.T. Liu, *J. of Materials Science,* 41 (2006) 5001
11. H.Guo, G. F. Li, X.Cai, J. of *Materials Science and Technology,* 21 (2005) 459
12. H.Guo, G. F. Li., X.Cai, Key. *Engineering Materials,* 2501(2005) 297
13. J.Q. Han, E.H. Zhu, Z.Y.Ke "Stress corrosion cracking of X-70 pipeline steel in near-neutral pH soil solution", Proc. of the Bienal International Pipeline Conference, (2004) 167
14. B.T. Lu, J.L. Luo, *Corrosion*, 62 (2006) 129
15. J.Q. Wang, A. Atrens, *Corros. Sci,* 45(2003) 2199
16. S.L. Asher, B. Leis, J. Colwell *Corrosion*, 63 (2007) 952
17. R. Chu, W. Chen, S.H. Wang, F. King, T.R. Jack, R.R. Fessler, *Corrosion* 60 (2004) 275
18. D.X. He, W. Chen, J.L. Luo, *Corrosion*, 60 (2004) 779
19. M.A.V. Devanathan, Z. Stachurski, *Proc. Roy. Soc. London,* A 270(1962) 90
20. R.N. Parkins, "The Controlling Parameters in Stress Corrosion Cracking", Fifth Symposium on Line Pipe Research, L30174 (Arlington, VA:AGA, 1974).
21. R.N. Parkins, *Corrosion,* 52(1996) 363
22. J.P. Hirth, *Metallurgical Transactions,* 11A (1980) 861